Published in final edited form as:
Int J Radiat Oncol Biol Phys. 2008 September 1; 72(1): 278–287. doi:10.1016/j.ijrobp.2008.05.014.

4D CT-based Treatment Planning for Intensity-Modulated Radiation Therapy and Proton Therapy for Distal Esophagus Cancer

Xiaodong Zhang, PH.D.[*], **Kuai-Le Zhao, M.D.**[‡], **Thomas M. Guerrero, M.D.**[†], **Sean E. McGuire, M.D.,PH.D.**[†], **Brian Yaremko, M.D.**[†], **Ritsuko Komaki, M.D.**[†], **James D. Cox, M.D.**[†], **Zhouguang Hui, M.D.**[*], **Yupeng Li, M.S.**[*], **Wayne D. Newhauser, PH.D.**[*], **Radhe Mohan, PH.D.**[*], and **Zhongxing Liao, M.D.**[†]

[*]*Department of Radiation Physics, The University of Texas M. D. Anderson Cancer Center, Houston, TX*

[‡]*Department of Radiation Onocology, Fudan University Cancer Hospital, Shanghai, People's Republic of China*

[†]*Department of Radiation Oncology, The University of Texas M. D. Anderson Cancer Center, Houston, TX*

Abstract

Purpose—To compare three-dimensional (3D) and 4D computed tomography (CT)– based treatment plans for proton therapy or intensity-modulated radiation therapy (IMRT) for esophageal cancer in terms of doses to the lung, heart, and spinal cord and variations in target coverage and normal tissue sparing.

Materials and Methods—IMRT and proton plans for 15 patients with distal esophageal cancer were designed from the 3D average CT scans and then recalculated on 10 4D CT data sets. Dosimetric data were compared for tumor coverage and normal tissue sparing.

Results—Compared with IMRT, median lung volumes exposed to 5,10, and 20 Gy and mean lung dose were reduced by 35.6%, 20.5%,5.8%, and 5.1 Gy for a two-beam proton plan and by 17.4%, 8.4%,5%, and 2.9 Gy for a three-beam proton plan. The greater lung sparing in the two-beam proton plan was achieved at the expense of less conformity to the target (conformity index CI=1.99) and greater irradiation of the heart (heart-V40=41.8%) compared with the IMRT plan(CI=1.55, heart-V40=35.7%) or the three-beam proton plan (CI=1.46, heart-V40=27.7%). Target coverage differed by more than 2% between the 3D and 4D plans for patients with substantial diaphragm motion in the three-beam proton and IMRT plans. The difference in spinal cord maximum dose between 3D and 4D plans could exceed 5 Gy for the proton plans partly owing to variations in stomach gas-filling.

Conclusions—Proton therapy provided significantly better sparing of lung than did IMRT. Diaphragm motion and stomach gas-filling must be considered in evaluating target coverage and cord doses.

Correspondence and reprint requests to: Zhongxing Liao, M.D., Department of Radiation Oncolgy, The University of Texas, M.D. Anderson Cancer Center, Houston, TX 77030, Tel:713-563-2300, Fax: 713-563-2331, Email:zliao@mdanderson.org.

Conflict Interest: None

Keywords

esophagus; IMRT; proton; lung; radiotherapy

INTRODUCTION

Pulmonary complications are the most common serious morbidity after esophagectomy and are the leading cause of postoperative mortality among patients treated with surgery for esophageal cancer. The incidence of postoperative pulmonary complications is 30% (1) and pulmonary complications are responsible for 55% of in-hospital deaths (2). Recent studies indicate that radiation exposure to lung may have a greater impact on postoperative pulmonary complications than do other clinical factors (3). Wang et al. (4) found that the volume of the lung spared from doses of 5 Gy or higher was the only independent predictive factor associated with postoperative pulmonary complications for patients with esophageal cancer treated with concurrent chemoradiotherapy followed by surgery. These findings, in combination with a report from Guerrero et al. (5) that the uptake of fluorodeoxyglucose (FDG) in normal lung after low-dose irradiation has a linear relationship with the dose received, underscore the importance of reducing the volume of lung that receives doses as low as 5 Gy.

The effects of radiation therapy on the heart have well been documented in patients with breast cancer and lymphoma. (6,7). For esophageal patients, Gayed et. al. found that radiaton was associated with a high prevalence inferior left ventricular ischemia detected by myocardial perfusion abnormalities on cardiac gated myocardial perfusion imaging (GMPI) (8). Importantly, most perfusion defects were encompassed within an isodose line greater than 45 Gy in RT plan. The objectives of the current treatment strategy at our institution are local control, balancing doses to the lung and the heart, and limiting the point spinal cord dose to less than 45 Gy. In addition to avoiding pulmonary complications, preserving heart function is seen as increasingly important. However, it is often difficult to decrease the heart dose without jeopardizing the dose distribution in the tumor or increasing the doses to other structures such as lungs and spinal cord.

Recent advances in photon treatment planning and delivery techniques, such as three-dimensional conformal radiation therapy (3D CRT) and intensity-modulated radiation therapy (IMRT), have led to improved radiation dose distribution and reduced exposures to the lungs and other surrounding normal tissues. Chandra et al. (9) studied the feasibility of using IMRT to improve lung sparing in patients with distal esophageal cancer. They demonstrated with treatment planning comparisons that IMRT reduced the V10, the V20, and the mean lung dose. However, another study by Nutting et al. (10) indicated that using IMRT conferred only a small benefit in terms of lung sparing as compared with 3D CRT.

Further improvements in normal tissue sparing can be accomplished with proton therapy, which has fundamental physical advantages over photon beams (11–13). In particular, proton beams have sharp lateral penumbrae, finite penetration ranges, and can be spread and shaped laterally and in depth (14). These characteristics allow proton beams to deliver large and uniform doses to the tumor while sparing nearby normal tissues. Several investigators have documented the clinical benefit of protons in the treatment of esophageal tumors. In one such study, Sugahara et al. (15) escalated doses to the primary tumor to 80 Gy by using proton beams. They reported that this approach led to 5-year survival rates of 55% for patients with T1 tumors and 13% for those with T2–T4 tumors.

Proton beam therapy for distal esophageal cancers is challenging because of the respiratory motion of the tumor, esophagus, diaphragm, heart, stomach, and lungs. Traditionally, treatment

planning is done with a single 3D CT scan, which can be either a free-breathing scan or a time-averaged result of a 4D CT scan. Respiratory motion during CT data acquisition can induce severe motion artifacts, resulting in inaccurate assessment of organ shape and location, and hence using a single CT scan to design and evaluate the treatment plan may provide inaccurate information on the dose actually delivered to the patient (16,17). Numerous studies have shown that using a free-breathing or averaged CT scan to evaluate treatment plans is misleading; several groups (16,17) showed that the target dose was *apparently* covered in a 3D-CT–based proton plan, but the same treatment fields applied to a 4D-CT–based plan revealed severe under-dosage of the target. For these reasons, a more complete understanding of the effects of respiratory motion in treatment planning is needed in order to assess the role of proton beams in the treatment of distal esophageal cancer.

The aim of this study was to quantify the degree of lung volume sparing at different dose levels with proton therapy as compared with IMRT. We also sought to clarify the differences in these treatment techniques with regard to the doses to the lung, heart, and spinal cord. We investigated these effects by comparing treatment planning methods based on 3D CT versus 4D CT images.

MATERIALS AND METHODS

We retrospectively selected 15 cases from our institutional records to represent typical anatomies. All patients had tumors involving the distal esophagus and gastroesophageal junction. All patients had been treated with definitive intent using photon 3D CRT or IMRT with concurrent chemotherapy in our clinic, and all had provided both free-breathing CT images and 4D CT images.

CT imaging and target volume delineation

A 4D CT set was sequentially acquired for each patient by using a multislice scanner. The slice width was 2.5 mm. CT images were acquired first while the patient was free-breathing, with 4D images acquired immediately thereafter. During the 4D CT image acquisition, patient respiration was monitored with an external respiratory gating system (Real-Time Position Management Respiratory Gating System; Varian Medical Systems, Palo Alto, CA). After acquisition, the CT images were time-stamped and the corresponding respiratory phases were registered according to the externally-acquired respiratory signal. Each 4D CT data set consisted of 10 CT data sets representing 10 equally divided breathing phases in a complete respiratory cycle. The average CT was calculated from the mean CT number of the 10 CT data sets at each pixel location, respectively. The phase corresponding to 0% CT was denoted as T0 CT, which represents the end-of-inspiration CT; the 50% CT phase (T50 CT) represents the end-of-expiration CT. All other phases were in between these two extremes. The 4D CT images provided quantitative time-dependent 3D information about internal organ motion, allowing quantitative description of internal organ motion for both treatment targets and normal organs.

We term the 3D plan in this study as the plan designed and evaluated using the average 3D CT from the 4D CT. The target volumes in the 3D and 4D CT images were defined and delineated in a self-consistent manner in order to minimize biases in subsequent dose calculations. Gross tumor volumes were contoured on the end-of-expiration-phase CT (T50) from the 4D CT data, and then the contours were expanded to form the clinical target volume (CTV). The CTV contours were then propagated to the other nine respiratory phases by using an in-house deformable image registration algorithm (18). The volume of the CTV on all 10 CT phases was defined as the internal clinical target volume (ICTV) and was used as the target volume for treatment plan design. The lung, heart, and spinal cord were manually contoured on the averaged CT and on all 10 phases of the 4D CT. The 3D plan was developed by using the

averaged CT images for treatment planning. Then, utilizing the machine settings from the 3D plan, the dose distribution was calculated for each phase of 4D CT images. For each patient, each treatment plan was separately calculated for each of the ten respiratory phases.

Treatment planning methods

A commercially available treatment planning system (Eclipse; Varian Medical Systems, Inc., Palo Alto, CA)(19,20)was used to design both the IMRT and proton therapy plans. For each patient, two proton plans and one IMRT plan were designed. The first type of proton plan consisted of two beams from the anterior-posterior direction. The second type of proton plan consisted of three beams to best conform the dose to the target. For IMRT planning, each patient plan included five coplanar, 6-MV beams placed at gantry angles of 25, 60, 100, 150, and 220 degrees (according to the International Electrotechnical Commission scale).

The proton treatment plans in this study were designed based on a passive scattering beam delivery system.(19,20)This technique required a patient portal–specific collimating aperture to laterally conform the radiation field to the tumor. A range compensator was also used to conform the dose to the distal edge of the target; this device is designed to restore conformity that would otherwise be degraded by internal anatomic heterogeneities and external surface irregularities. The depth of the distal edge and proximal edge of the target volume determined the proton beam energy and the width of the spread-out Bragg peak. The choice of the major planning parameters (e.g., aperture margins, distal margins, proximal margins, smearing margins, and border smoothing margins) were approximated by using the method suggested by Moyers et al. (21). We chose ICTV as the target volume to account for uncertainties of internal organ motion. The aperture margin value used for all the proton beams in this study was 10 mm. The distal and proximal margins for all proton beams were approximated based on a 3.5% uncertainty for CT number accuracy. The smearing margin accounts for the internal organ motion, set-up error, and proton scatter. In this study, we set the smearing margin to 1 cm for the two-beam plans and to 0.5 cm for the three-beam plans. We deliberately chose the smaller smearing margin for the three-beam plans to see the effect of diaphragm motion on tumor coverage.

All proton and IMRT plans were normalized to provide the same coverage to the ICTV. All plans were designed to provide 99.5% coverage of the ICTV by the prescribed dose (50.4 Gy).

Plan evaluation

To compare plans with the different modalities and different beam arrangements, we calculated dose-volume histograms for the lungs (left, right and total), heart, and spinal cord. Organ volumes receiving doses of at least 5 Gy (V5), 10 Gy (V10), 20 Gy (V20), and 30 Gy (V30) were calculated for lungs (left, right, and total), the V40 and V50 for heart, and the maximum dose to the spinal cord were compared between the photon plan and the proton plans. The "volume spared" (VS_{dose}) (22), defined as total lung volume minus the absolute V_{dose}, was introduced to illustrate the volume of organ *not* exposed to a certain dose. The endpoints VS5, VS10, VS20, and VS30 were also calculated for lung. We also calculated the conformity index (CI) to the ICTV. The CI is defined as V_{DP}/V_{target}, where V_{DP} is the volume enclosed by the prescribed isodose surface (i.e., the prescribed dose) and V_{target} is the volume of the ICTV. Higher CI values indicate lower conformity of the dose distribution to the target volume.

The treatment plans were evaluated on both the 3D and 4D CT scans. Because contours had already been delineated on each phase of the 4D CT images, for the purposes of this study we calculated the volume receiving the indicated dose or higher for the ICTV, lung, heart and spinal cord. We then averaged these volumes over all ten phases to define an appropriate metric for evaluation of 4D CT based plans.

Statistical analysis was done with pairwise Wilcoxon signed-rank tests. The significance level was set as $p \leq 0.05$ (two-tailed tests).

RESULTS

Endpoints of IMRT, two-beam, and three-beam proton plans calculated using 3D CT images

The dose distributions of the IMRT photon plan and the two proton plans for patient 13 are presented in Figure 1. Limitations incurred by the physical characteristics of the photons resulted in considerable spread in the low-dose isodose lines (e.g., 20 Gy and 10 Gy) in the IMRT plan. In contrast, the two-beam proton plan showed minimal spread of the 20 Gy and 10 Gy isodose lines in the lungs. However, this lung sparing was achieved at the expense of reduced conformity of dose to the ICTV: the CI for the two-field proton plan was 1.98, as compared with 1.54 for the IMRT plan. The three-field proton plan improved the dose conformity to the ICTV (CI = 1.45) and was comparable to that of the IMRT plan (1.54). However, the three-beam proton plan irradiated a larger volume of the right lung than did the two-beam proton plan.

Figure 2 compares the dose-volume histogram data from the IMRT plan and the two- and three-beam proton plans. The falloffs of the dose-volume histograms of ICTV in these three plans were quite similar, indicating comparable target homogeneity in the three plans. In regions receiving less than 25 Gy, both the two- and three-beam proton plans spared lung tissue to a much greater extent than did the IMRT plan. At 20 Gy, lung sparing was comparable in the two- and three-beam proton plans. However, below 20 Gy the two-beam proton plan spared much more of the lung than did the three-beam proton plan. In comparison with the IMRT plan, the three-beam proton plan showed a clear advantage in sparing the cord, but the two-beam proton plan did not. The IMRT plan provided better sparing of the heart at dose levels higher than 30 Gy than did the two- and three-beam proton plans, but in general the three-beam proton plan spared more of the heart than did the two-beam proton plan.

More detailed comparisons of the IMRT and proton plans are presented in Table 1. The average CI for the target in the IMRT plans was 1.55, compared with 1.99 in the two-beam proton plan ($p = 0.001$) and 1.46 in the three-beam proton plan ($p = 0.006$). The two-beam proton plan did not conform to the target as well as the IMRT plan or the three-beam proton plan did. Target conformity in the three-beam proton plan was similar to that in the IMRT plan.

According to the IMRT plans, median V5, V10, and V20 values for the lung were 49.5%, 32.5%, and 15.6%, respectively. Compared to the IMRT values, the two-beam proton plan provided reductions in median V5, V10, and V20 values of 35.6% ($p = 0.001$), 20.5% ($p = 0.001$), and 5.8% ($p = 0.001$), respectively. The three-beam proton plans revealed similar reductions (17.4% ($p = 0.001$), 8.5% ($p = 0.001$), and 5% ($p = 0.053$), respectively). Compared to the mean lung dose of 9.65 Gy from the IMRT plans, the two- and three-beam proton plans provided reductions in mean lung doses of 5.1 Gy and 3.0 Gy, respectively. In the IMRT plans, the median lung volume spared at 5 Gy (VS5) was 1815 cm^3; the VS10 was 2598 cm^3; and the VS20 was 3024 cm^3. The two-beam proton plans increased the median VS5, VS10, and VS20 values by 1238 cm^3 ($p = 0.001$), 498 cm^3 ($p = 0.001$) and 126 cm^3 ($p = 0.001$), respectively. The three-beam proton plans also increased the median VS5, VS10, and VS20 values (by 717 cm^3 ($p = 0.001$), 236 cm^3 ($p = 0.001$), and 78 cm^3 ($p = 0.001$), respectively), but those benefits were smaller than those achieved with the two-beam proton plan.

The mean total body dose in the IMRT plan (9.1 Gy) was considerably higher than that in the two-beam proton plan (5.7 Gy) or the three-beam proton plan (5.9 Gy), a difference in integral dose of approximately by a factor of 1.6. Interestingly, no difference in total body mean dose

was found between the two-beam and three-beam proton plans, suggesting that increasing the number of beams used in the proton plan did not increase the integral dose.

In terms of maximum dose to the spinal cord, no differences were found between two-beam proton plan and the IMRT plan, which were both about 40 Gy; however, that dose in the three-beam proton plan, 25.6 Gy, represented a reduction of 15.5 Gy ($p = 0.001$). The heart V40 and V50 values for the two-beam proton plan were 41.8% ($p = 0.02$) and 28.6% ($p = 0.002$), respectively, which were higher than the corresponding 35.7% and 15% values for the IMRT plan. The V40 in the three-beam proton (27.7%) was significantly ($p = 0.002$) lower than that in the IMRT plan; however, at 15.9%, the V50 for the three-beam proton plan was no different from the V50 for the IMRT plan ($p = 0.125$).

Differences in endpoints for IMRT, two-beam, and three-beam proton plans calculated using 3D vs 4D CT images

The differences between the values calculated using 4D CT and 3D CT images for the IMRT plans and the two-beam and three-beam proton plans are listed in Table 2. The CIs were not sensitive to the CT datasets used for all the plans. Tumor coverage, as assessed by the ICTV receiving the prescribed dose, was adequate in the two-beam proton plan for all patients. However, the largest differences in the ICTV receiving the prescribed doses between the 3D and 4D scan data were 8.7% for the IMRT plan and 3.9% for the three-beam proton plan. These large differences were present in a single case (patient 14) in both the IMRT and three-beam proton plans.

Although they were not different statistically, the V5, V10, and lung mean doses for the IMRT plans and the two-beam proton plans calculated with the 4D CT data were lower than those calculated with the 3D CT data. However, the V5, V10, and mean lung dose for three-beam proton plans calculated with 4D CT were larger than those calculated using the averaged (3D) CT. Nevertheless, the average differences in lung endpoints calculated with 4D CT images were all less than 0.5% (for volumes) or 3 cGy (for mean dose).

No significant difference was found in the maximum dose to the spinal cord from the IMRT plans calculated from the 4D CT scans versus the 3D CT scans. However, the maximum cord doses calculated with the 4D CT data were 1.06 Gy and 1.38 Gy—higher than those calculated with 3D CT data for both the two-beam ($p = 0.14$) and the three-beam ($p = 0.86$) proton plans. The doses received by 1% of the spinal cord calculated using the 4D CT data were 1.76 Gy ($p = 0.02$) (in the two-beam plan) and 0.59 Gy (in the three-beam plan) ($p = 0.01$), both higher than the doses calculated with 3D CT. For some patients, the difference in maximum cord dose (calculated from 3D vs 4D CT image data) reached 5.19 Gy in the two-beam proton plan and 6.22 Gy in the three-beam proton plan.

Differences in heart V40 and V50 as calculated with the 4D CT and 3D CT data were small and the differences between these values for the IMRT and proton plans were not statistically significant.

Correleration between tumor motions and differences in endpoints calculated using 3D vs 4D CT images

The amplitude of tumor motion in each of the 15 patients is shown in Figure 3a. That amplitude exceeded 1 cm in six patients (patients 3, 5, 7, 8, 11, and 14) and reached 2.4 cm in one (patient 14). Differences in the percentage of ICTV receiving the prescribed dose in each of the three treatment plans (Figure 3b) were less than 1% for all of the two-beam proton plans but exceeded 1% for patients 5, 8, 10, and 15 for the IMRT plan and for patients 5, 7, and 15 for the three-beam proton plan. The ICTV receiving the prescribed dose in patient 14, evaluated with the

4D CT data, was much lower than the value evaluated with the single 3D CT in both the IMRT and the three-beam proton plans, perhaps because the magnitude of tumor motion for this patient reached 2.43 cm. For patient 8, differences in the ICTV receiving the prescribed dose calculcated using the 4D CT vs the single CT data were 2.2% for IMRT and 0.3%% for the three-beam proton plans, suggesting that for this patient, the IMRT plan was influenced more by uncertainties on CT scans than was the three-beam proton plan. However, the corresponding differences for patient 7 were –0.03% and 2.06%, suggesting that three-beam proton plan was affected more by CT uncertainties than was the IMRT plan. Differences in the lung endpoints V5 and lung mean dose between the 4D and 3D plans are shown in Figures 3c and 3d. Only two patients (patients 7 and 14) exhibited large differences in these lung endpoints. The maximum dose to the cord was equal in the IMRT plans based on 4D CT and those based on 3D CT images (Figure 3e). In contrast, significant differences in the maximum cord dose were observed in proton therapy plans between 3D and 4D plans; specifically, this difference exceeded 1.5 Gy (patients 1, 5, 6, 7, and 11) for the two-beam proton plan and (patients 7, 9, 11, and 14) for the three-beam proton plan (Figure 3e). Differences in heart V40 between the 3D and 4D CT data sets (Figure 3f) seemed to be random in both the IMRT and the proton plans.

DISCUSSION

Clinical studies have shown that minimizing the lung volume irradiated even to very low doses can result in fewer pulmonary complications (4). When we compared our findings on the volume of lung spared from 5 Gy (VS5) with recent clinical data available for the patients studied here, the lung sparing in the two- and three-beam proton plans could potentially reduce the probability of pulmonary complications from 18.5% (8.6%, 40.9%) with IMRT to 5% (0%, 19.9%) and 11% (2.5%, 25.4%) with the two-beam and three-beam proton plans.

Clinical experience with proton therapy in Japan indicates that escalating the dose to as high as 80 Gy can improve local control in esophageal cancer (15,23). At the M. D. Anderson Cancer Center, the tolerance spinal cord dose is normally 45 Gy. In the study reported here, the maximum dose to the cord for the two-beam proton plan was about 40 Gy, approaching the tolerance dose limit. On the assumption that the cord is the dose-limiting organ, only a small dose escalation would be possible with the two-beam proton technique. In contrast, the three-beam proton technique seems to allow substantial dose escalation because the maximum cord doses in this study were only 25.6 Gy.

In our experience, the time and effort spent in treatment planning for patients with lung cancer are less for proton therapy than for IMRT. In the current study, the typical time needed to design an IMRT plan was 3 hours vs 20 minutes for a proton plan. Proton plans were also easier to customize to accommodate patient-specific dose constraints on various normal tissues, such as reducing the dose to the normal lung tissue at the expense of higher dose to the heart. As an example of this customization process, Figure 4a illustrates the beam settings for a three-beam proton plan for patient 13. The original relative weights of the proton beams were 1, 0.5, and 0.2 for beam angles of 0, 210, and 110 degrees, respectively. Simply changing these beam weights to 1, 2, and 1 led to better sparing of the heart than in the IMRT plans (Figure 4b). However, this better sparing of the heart was achieved at the expense of more dose to the lung (Figure 4b, blue lines). This design process involved minimum trial and error as compared with IMRT. The design process was also fast because changing the beam weights does not require redesigning the range compensator or calculating the unweighted doses from individual beams. Recent treatment planning studies (24) of lung cancer suggest that this type of customization may be more time-consuming and complex for IMRT, because it potentially involves non-coplanar beam angle optimization.

Because protons are quite sensitive to density changes along their path (25), evaluating a proton-therapy treatment plan by using the full 4D CT provides a way of evaluating the dosimetric impact of the respiration motion. For example, Figure 5 shows averaged CT slices (for the planning CT) and 4D CT at T50 phase for patient 14. Notably, liver and stomach were not visible in the planning CT but were in the T50 phase CT image because of diaphragm motion. For three-beam proton plan, the liver and stomach were in and out the beam path because of diaphragm motion. The consequences of this motion are apparent in the panels at right on Figure 5, in which the T50 phase images reveal severe underdosing of the ICTV in this patient in both the three-beam proton plan and the IMRT plan, although the averaged planning CT indicated good coverage of the ICTV. We also observed rather alarming differences in ICTV coverage between the 3D and 4D plans for patients 5, 7, and 8. Evaluating the plan by using the 4D CT data set was important in terms of visualizing the effects of internal organ motion on the dose distribution and evaluation endpoints for both the IMRT and proton plans. For example, treatment plans for both IMRT and three-beam proton therapy may need to be redesigned for patients such as patient 14.

Finally, in this study, we found that the predicted maximum dose to the spinal cord from either of the two-beam or three-beam proton therapy plans was significantly different according to whether the plans were calculated based on 4D CT versus 3D CT images. However, for IMRT, the predicted maximum cord dose did not differ in the 3D versus the 4D plans. One reason for the 3D versus 4D differences in cord doses in the proton plans was that changes in the amount of stomach gas in the various 4D CT scans resulted in large changes in the proton penetration depth. An example of dose distributions for the same plans calculated according to the averaged CT and the T0, T30, and T50 CT images is shown in Figure 6. Notably, in the original plan the prescription dose line (in yellow) is at least 2 cm away from the spinal cord, and that distance was about the same on the T0 scan. However, the prescription isodose lines touched the cord on the T30 and T50 scans, a direct result of different amounts of stomach gas being in the beam path. With a two-beam proton plan, the maximum cord dose from the 4D CT exceeded 45 Gy for three of the 15 patients (patients 5, 7, and 11), whereas cord dose was less than 45 Gy for all patients when 3D CT-based planning was utilized. In other words, a treatment plan that is acceptable in terms of cord dose based on a single CT scan may not be acceptable when based on 4D CT.

CONCLUSIONS

We demonstrated that two-beam proton plans consistently spared larger volumes of lung and reduced the mean dose to the lung. However, the gain in lung sparing achieved with the two-beam proton plan was offset somewhat by reduced conformity to the target and by higher radiation to the heart relative to the IMRT and three-beam proton plans. For the three-beam proton plans, target conformity was similar to that of the IMRT plans; lung sparing that was better than that with IMRT but worse than that with the two-beam proton plans; and heart sparing that was similar to that in the IMRT plans. For proton plans, range errors due to diaphragm motion and stomach gas-filling must be considered in evaluating target coverage and spinal cord dose. IMRT and three-beam proton plans based on a 3D CT scan could overestimate the target coverage. The 3D CT planning method could underestimate the maximum spinal cord dose when compared with the 4D CT method for proton planning.

Acknowledgments

This work was supported in part by grants from the National Cancer Institute (CA74043) and the Radiological Society of North America's Research and Education Foundation Program.

REFERENCES

1. Lin FCF, Durkin AE, Ferguson MK. Induction therapy does not increase surgical morbidity after esophagectomy for cancer. Annals of Thoracic Surgery 2004;78:1783–1789. [PubMed: 15511475]
2. Law S, Wong KH, Kwok KF, et al. Predictive factors for postoperative pulmonary complications and mortality after esophagectomy for cancer. Annals of Surgery 2004;240:791–800. [PubMed: 15492560]
3. Lee HK, Vaporciyan AA, Cox JD, et al. Postoperative pulmonary complications after preoperative chemoradiation for esophageal carcinoma: Correlation with pulmonary dose-volume histogram parameters. International Journal of Radiation Oncology Biology Physics 2003;57:1317–1322.
4. Wang SL, Liao ZX, Vaporciyan AA, et al. Investigation of clinical and dosimetric factors associated with postoperative pulmonary complications in esophageal cancer patients treated with concurrent chemoradiotherapy followed by surgery. International Journal of Radiation Oncology Biology Physics 2006;64:692–699.
5. Guerrero T, Castillo R, Noyola-Martinez J, et al. Reduction of pulmonary compliance found with high-resolution computed tomography in irradiated mice. International Journal of Radiation Oncology Biology Physics 2007;67:879–887.
6. Girinsky T, Pichenot C, Beaudre A, et al. Is intensity-modulated radiotherapy better than conventional radiation treatment and three-dimensional conformal radiotherapy for mediastinal masses in patients with Hodgkin's disease, and is there a role for beam orientation optimization and dose constraints assigned to virtual volumes? International Journal of Radiation Oncology Biology Physics 2006;64:218–226.
7. Prosnitz RG, Chen YH, Marks LB. Cardiac toxicity following thoracic radiation. Seminars in Oncology 2005;32:S71–S80. [PubMed: 16015539]
8. Gayed IW, Liu HH, Yusuf SW, et al. The prevalence of myocardial ischemia after concurrent chemoradiation therapy as detected by gated myocardial perfusion imaging in patients with esophageal cancer. Journal of Nuclear Medicine 2006;47:1756–1762. [PubMed: 17079807]
9. Chandra A, Guerrero TM, Liu HH, et al. Feasibility of using intensity-modulated radiotherapy to improve lung sparing in treatment planning for distal esophageal cancer. Radiotherapy and Oncology 2005;77:247–253. [PubMed: 16298001]
10. Nutting CM, Bedford JL, Cosgrove VP, et al. A comparison of conformal and intensity-modulated techniques for oesophageal radiotherapy. Radiotherapy and Oncology 2001;61:157–163. [PubMed: 11690681]
11. Goitein M, Lomax AJ, Pedroni ES. Treating cancer with protons. Physics Today 2002;55:45–50.
12. Isacsson U, Lennernas B, Grusell E, et al. Comparative treatment planning between proton and x-ray therapy in esophageal cancer. International Journal of Radiation Oncology Biology Physics 1998;41:441–450.
13. Smith AR. Intensity-modulated conformal radiation therapy and 3-dimensional treatment planning will significantly reduce the need for therapeutic approaches with particles such as protons - Against the proposition. Medical Physics 1999;26:1187–1187.
14. Pedroni E, Bacher R, Blattmann H, et al. The 200-Mev Proton Therapy Project at the Paul-Scherrer-Institute - Conceptual Design and Practical Realization. Medical Physics 1995;22:37–53. [PubMed: 7715569]
15. Sugahara S, Tokuuye K, Okumura T, et al. Clinical results of proton beam therapy for cancer of the esophagus. International Journal of Radiation Oncology Biology Physics 2005;61:76–84.
16. Engelsman M, Rietzel E, Kooy HM. Four-dimensional proton treatment planning for lung tumors. International Journal of Radiation Oncology Biology Physics 2006;64:1589–1595.
17. Kang Y, Zhang X, Chang JY, et al. 4D Proton treatment planning strategy for mobile lung tumors. International Journal of Radiation Oncology Biology Physics 2007;67:906–914.
18. Wang H, Dong L, Lii MF, et al. Implementation and validation of a three-dimensional deformable registration algorithm for targeted prostate cancer radiotherapy. International Journal of Radiation Oncology Biology Physics 2005;61:725–735.
19. Li Y, Zhang X, Lii M, et al. Incorporating partial shining effects in proton pencil-beam dose calculation. Physics in Medicine and Biology 2008;53:605–616. [PubMed: 18199905]

20. Newhauser W, Fontenot J, Zheng Y, et al. Monte Carlo simulations for configuring and testing an analytical proton dose-calculation algorithm. Physics in Medicine and Biology 2007;52:4569–4584. [PubMed: 17634651]

21. Moyers MF, Miller DW, Bush DA, et al. Methodologies and tools for proton beam design for lung tumors. International Journal of Radiation Oncology Biology Physics 2001;49:1429–1438.

22. Wang SL, Liao ZX, Wei X, et al. Analysis of clinical and dosimetric factors associated with treatment-related pneumonitis (TRP) in patients with non-small-cell lung cancer (NSCLC) treated with concurrent chemotherapy and three-dimensional conformal radiotherapy (3D-CRT). International Journal of Radiation Oncology Biology Physics 2006;66:1399–1407.

23. Koyama S, Tsujii H. Proton beam therapy with high-dose irradiation for superficial and advanced esophageal carcinomas. Clinical Cancer Research 2003;9:3571–3577. [PubMed: 14506143]

24. Chapet O, Khodri M, Jalade P, et al. Potential benefits of using non coplanar field and intensity modulated radiation therapy to preserve the heart in irradiation of lung tumors in the middle and lower lobes. Radiotherapy and Oncology 2006;80:333–340. [PubMed: 16934354]

25. Mackie TR. Intensity-modulated conformal radiation therapy and 3-dimensional treatment planning will significantly reduce the need for therapeutic approaches with particles such as protons - For the proposition. Medical Physics 1999;26:1185–1186. [PubMed: 10435517]

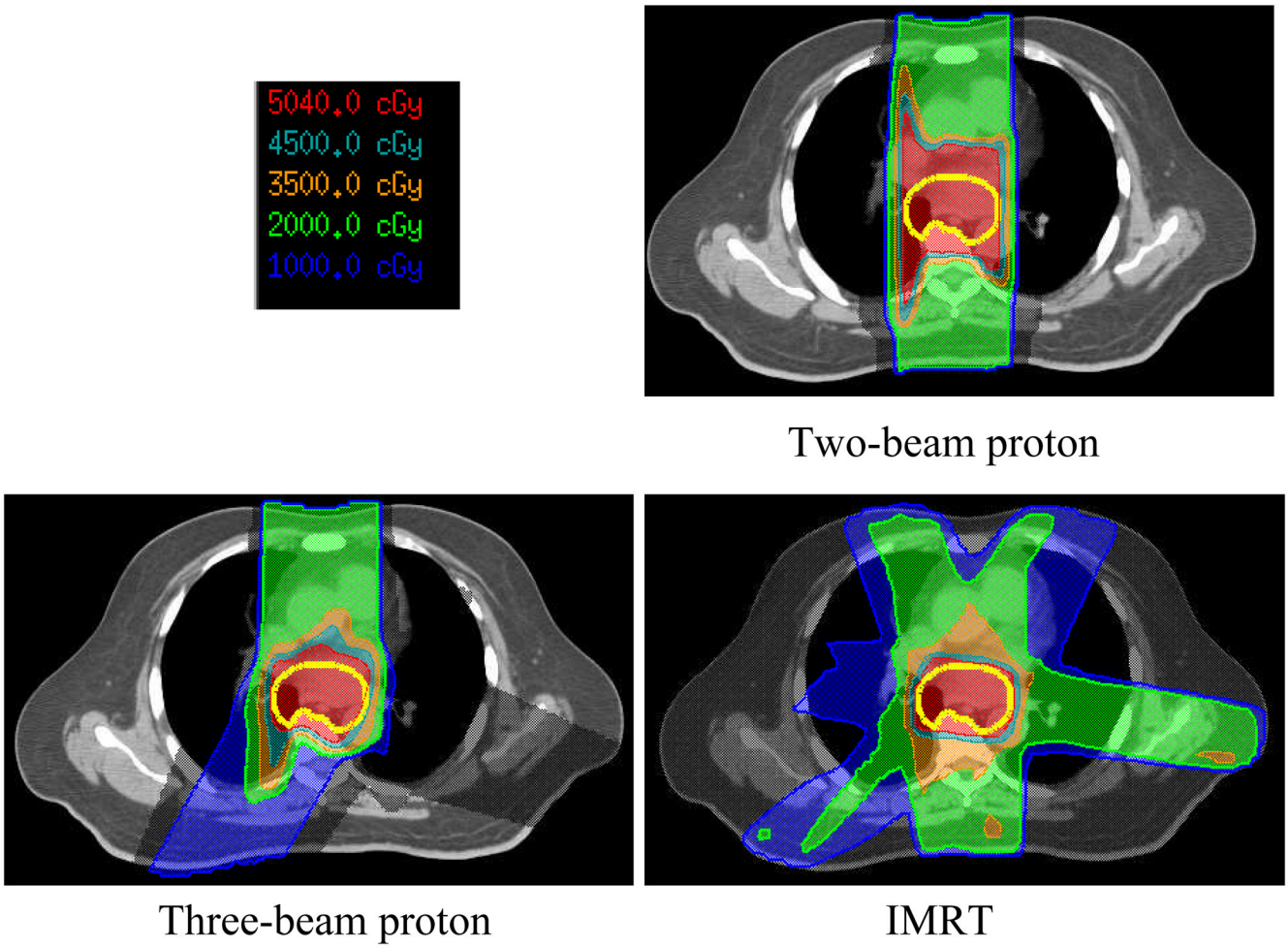

Fig. 1.
Transverse views of the dose distributions in the photon intensity-modulated radiation therapy (IMRT) plan and the two- and three-beam proton plans for patient 13. The thick yellow lines delineate the internal clinical target volume (ICTV).

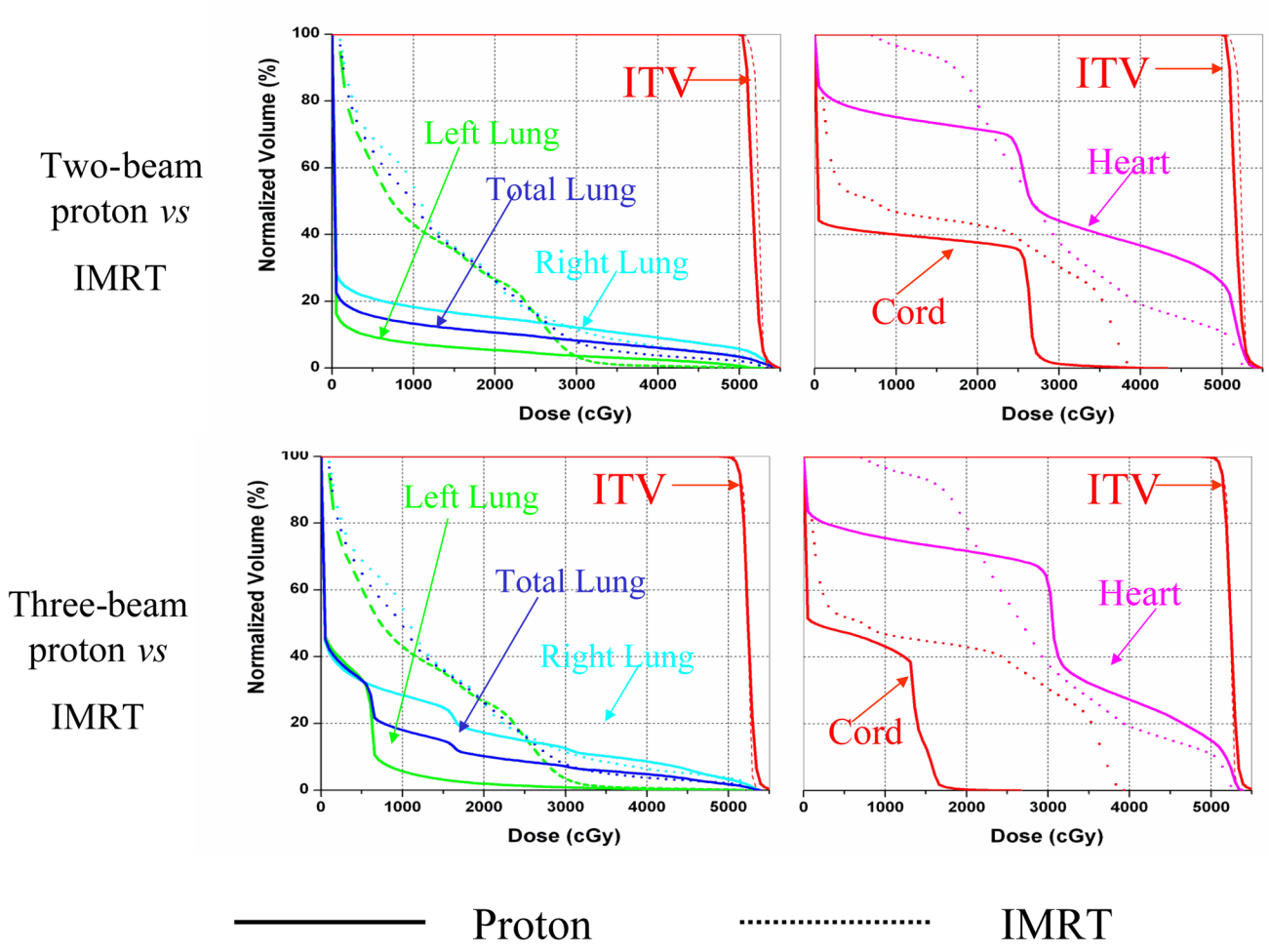

Fig. 2.
Comparisons from dose-volume histograms for the photon intensity-modulated radiation therapy (IMRT) plan (dashed lines) and the proton plan (solid lines) for patient 13.

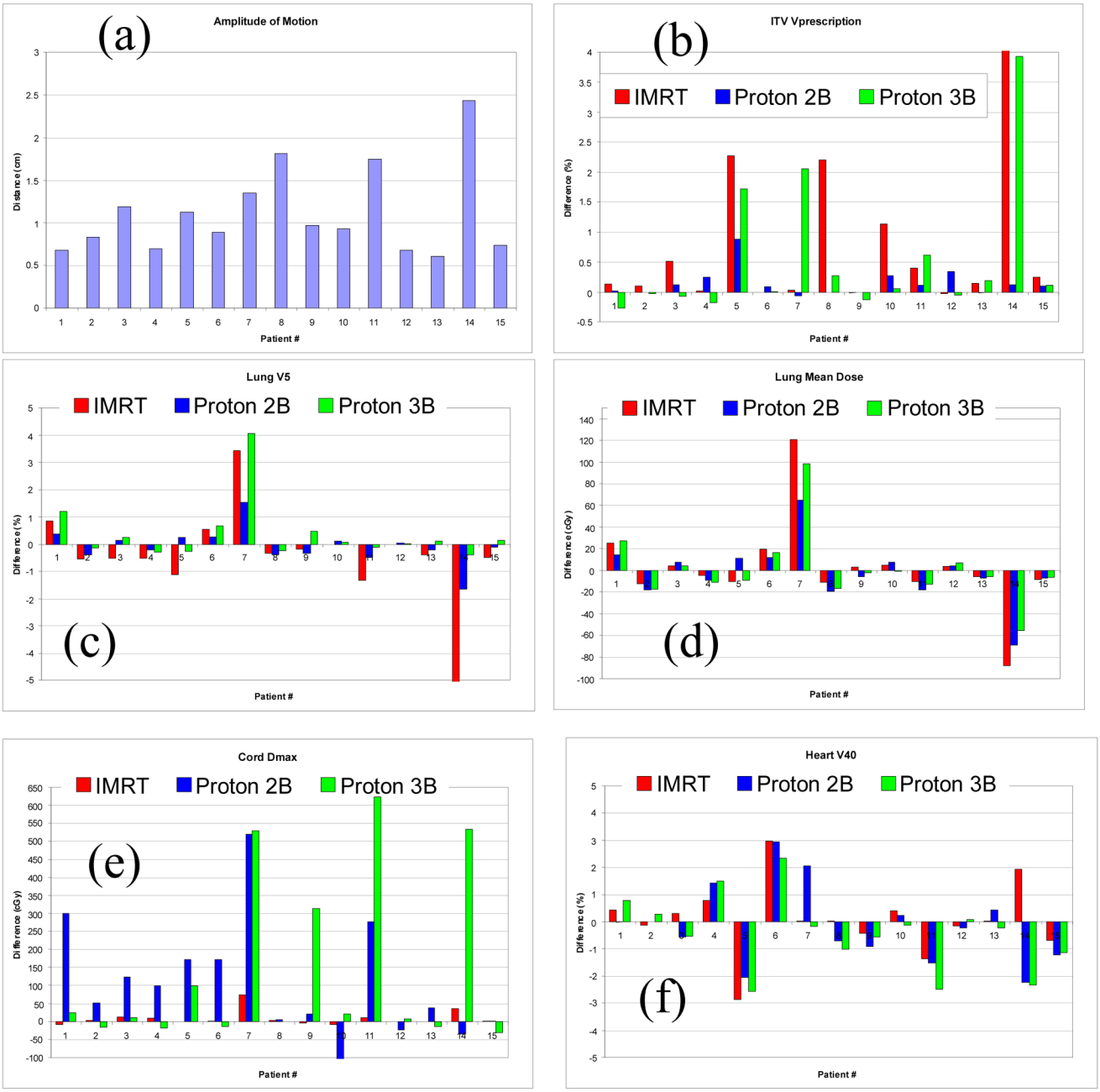

Fig. 3.

The amplitude of tumor motion (panel a) and differences in the endpoints in plans calculated with 4D CT versus single CT for the prescribed dose to the ICTV (b), the lung V5 (c), the lung mean dose (d), the cord maximum dose (e), and the heart V40 (f) for IMRT and for the two-beam and three-beam proton plans. IMRT, intensity-modulated radiation therapy; Proton 2B, two-beam proton therapy; Proton 3B, three-beam proton therapy.

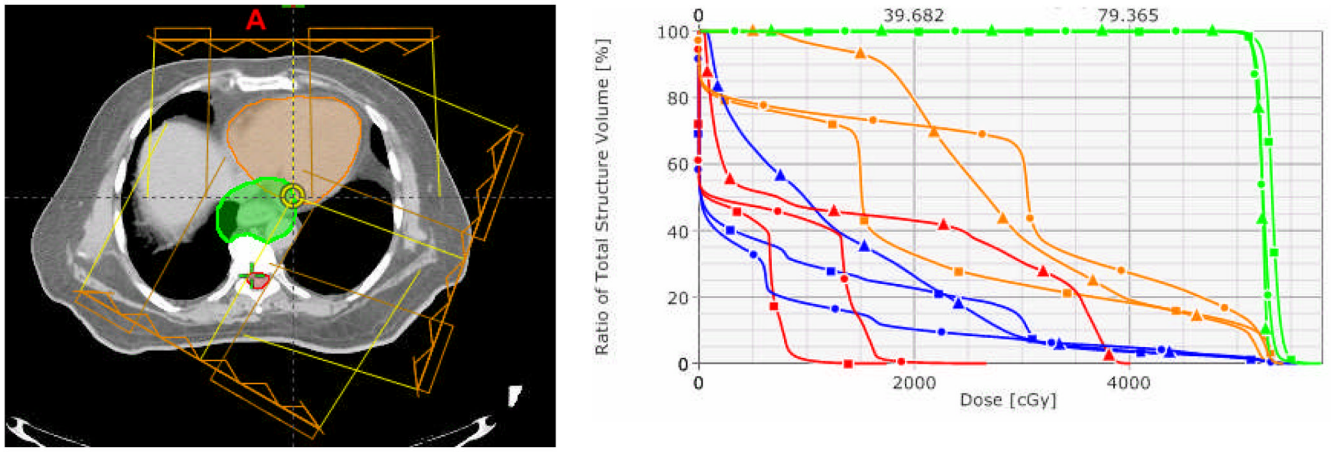

Fig. 4.

The effect of beam weighting on heart sparing for the three-beam proton plan for patient 13. Panel at left shows beam arrangement; 0, 110, and 210 refer to the beam angles (in degrees). Panel at right shows dose-volume histograms of three-beam plans using beam weights of 1, 0.2, 1 (circles) or 1, 2, 1 (squares), and IMRT plan (triangles). The green, blue, orange and red colors denote ICTV, total lung, heart and spinal cord.

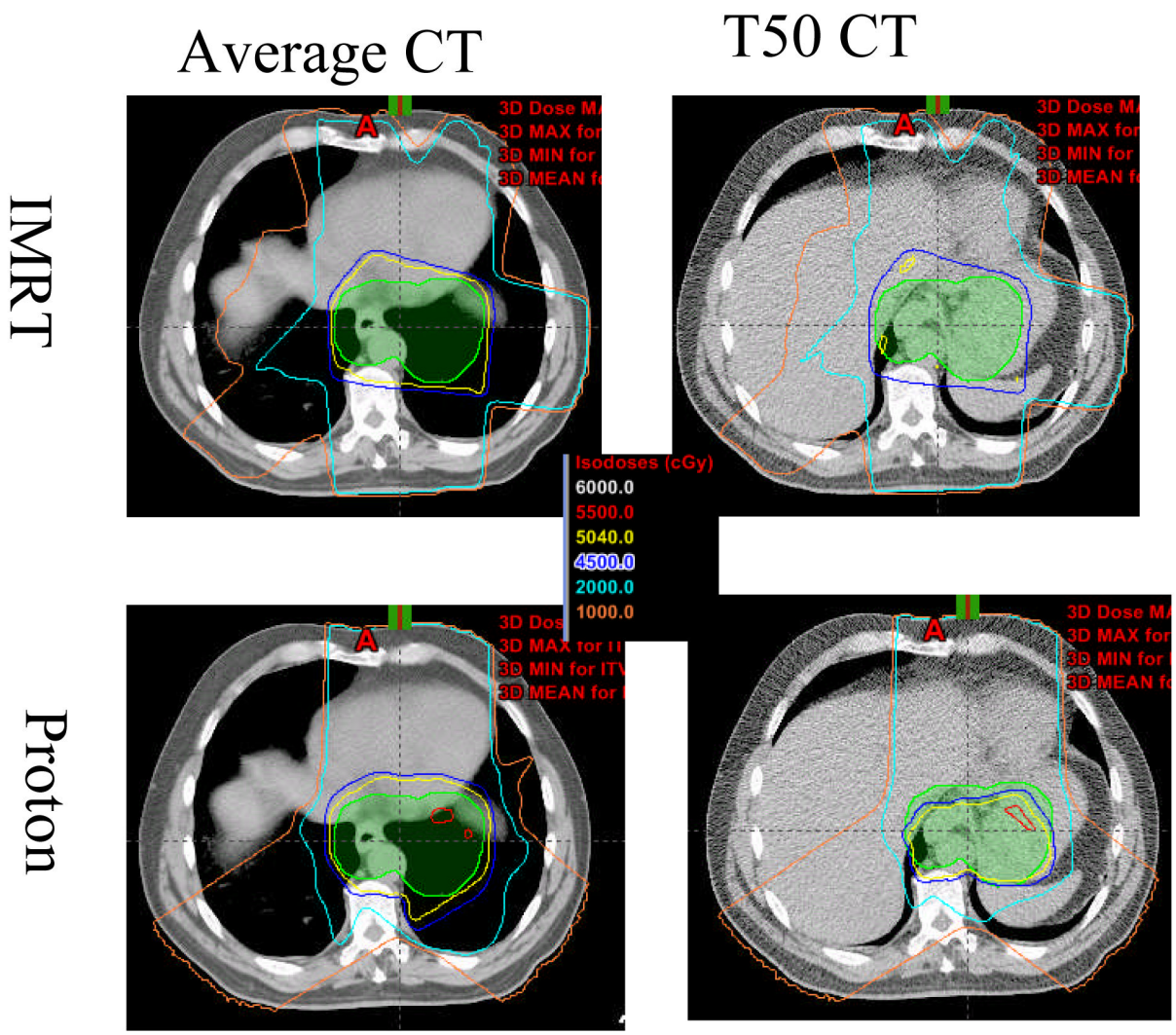

Fig. 5.

The effects of diaphragmatic motion on the dose distribution for patient 14 in the intensity-modulated radiation therapy (IMRT) plan (upper panels) and the three-beam proton plan (bottom panels). The panels at left show the dose distribution on the averaged CT; the panels at right show the dose distribution on the T50 phase of the 4D CT.

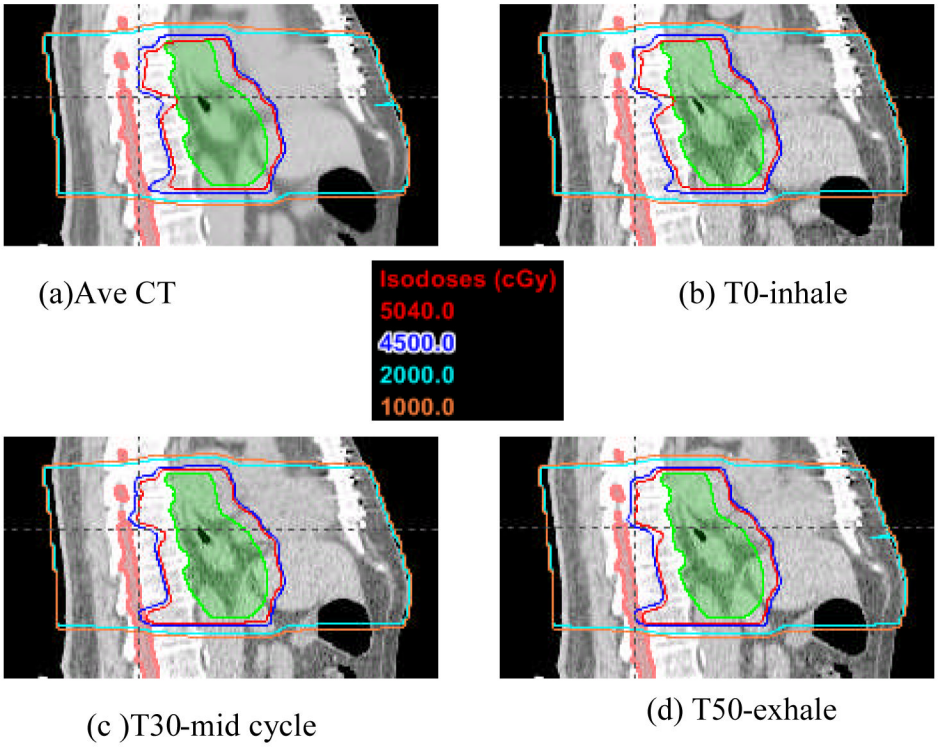

Fig. 6.
The effects of differences in stomach gas filling on dose distribution on an averaged CT scan (a), a T00 phase scan (b), a T30 phase scan (c), and a T50 phase scan (d) from 4D CT.

Table 1

Medians and ranges of endpoint values in the IMRT and the two- and three-beam proton plans

Endpoint	IMRT [Median (min, max)]	Two-Beam Proton Therapy	*P* Value vs IMRT	Three-Beam Proton Therapy	*P* Value vs IMRT
Conformity index	1.55 (1.44, 1.68)	1.99 (1.79, 2.28)	0.001	1.46 (1.36, 1.71)	0.006
Lung					
V5, %	49.5 (34.3, 65.1)	13.9 (6.9, 21.4)	0.001	32.1 (21.2, 41.6)	0.001
V10, %	32.5 (21.1, 49.3)	12.0 (5.7, 18.7)	0.001	24.1 (11.0, 35.8)	0.001
V20, %	15.6 (9.54, 26.3)	9.79 (4.34, 15.6)	0.001	10.6 (5.47, 16.5)	0.001
V30, %	7.08 (3.23, 10.88)	7.17 (2.78, 13.24)	1.000	6.61 (3.15, 10.4)	0.053
Mean dose, cGy	965.0 (680.4, 1305.36)	453.3 (201.6, 740.88)	0.001	664.6 (438.5, 937.4)	0.001
VS5, cm^3	1815 (643, 2491)	3053 (1553, 4306)	0.001	2532 (1233, 3225)	0.001
VS10, cm^3	2598 (933, 3216)	3096 (1596, 4433)	0.001	2834 (1508, 3475)	0.001
VS20, cm^3	3024 (1357, 4260)	3150 (1644, 4584)	0.001	3102 (1652, 4508)	0.001
VS30, cm^3	3226 (1697, 4741)	3271 (1688, 4836)	0.57	3277 (1708, 4859)	0.05
Cord, maximum dose, cGy	4107 (3691, 4349)	4035 (2963, 4480)	0.865	2563 (1053, 3971)	0.001
Heart					
V40, %	35.7 (16.7, 55.3)	41.8 (24.7, 66.2)	0.02	27.7 (13.9, 51.7)	0.002
V50, %	15.0 (7.07, 25.0)	28.6 (17.1, 46)	0.001	15.9 (8.2, 31.4)	0.125
Total body, mean dose, cGy	905.2 (599.8, 1315.44)	571.9 (322.6, 972.7)	0.001	587.3 (342.7, 932.4)	0.001

IMRT, intensity-modulated (photon) radiation therapy; V5. volume (of lung) exposed to 5 Gy or more; VS5, volume (of lung) spared from exposure of 5 Gy or more.

Table 2

Differences in medians and ranges of endpoint values in the IMRT and the two- and three-beam proton plans calculated from 3D CT vs 4D CT treatment planning data

Endpoint	IMRT [Median, (min, max)]	*P* Values [vs 3D, 2B proton, 3B proton]			Two-Beam Proton Therapy	*P* Values [vs 3D., 3B proton]		Three-Beam Proton Therapy	*P* Value [vs 3D]
Prescribed dose coverage	−1.06 (−8.7, 0.03)	0.003	0.03	0.05	−0.15 (−0.88, 0.06)	0.01	0.6	−0.55 (−3.93, 0.26)	0.17
Conformity index	−0.01 (−0.04, 0.03)	0.01	0.01	0.01	−0.01 (−0.08, 0.09)	0.001	0.001	−0.01 (−0.11, −0.01)	0.04
Lung									
V5,%	−0.43 (−5.9, 3.4)	0.17	0.16	0.46	−0.07 (−1.65, 1.52)	0.001	0.46	0.4 (−0.3, 4.1)	0.01
V10,%	−0.12 (−3.29, 3.23)	0.5	0.3	0.6	−0.04 (−1.5, 1.5)	0.07	0.5	0.14 (−1.0, 3.92)	0.04
V20,%	0.18 (−1.5, 3.3)	0.1	0.78	0.95	−0.01 (−1.41, 1.4)	0.003	0.33	−0.14 (−1.69, 1.18).	0.01
V30,%	0.21 (−0.69, 2.54)	0.003	0.19	1.0	−0.01 (−1.21, 1.28)	0.001	0.21	−0.16 (−1.34, 1.05)	0.05
Mean dose, cGy	−2.04 (−88.2, 120)	0.25	0.6	0.69	−2.01 (−68, 65)	0.18	0.49	1.08 (−55, 94)	0.17
Spinal cord									
d1, cGy	1.05 (−96.3, −11.3)	0.001	0.03	0.001	176(−11, 828)	0.02	0.01	59 (−21, 229)	0.01
Maximum dose, cGy	8.63 (−9, 74.6)	0.02	0.10	0.02	106 (−126, 519)	0.14	0.13	138 (−30, 622)	0.86
Heart									
V40,%	0.08 (−2.8, 2.9)	0.39	0.69	0.39	−0.16 (−2.23, 2.95)	0.11	0.21	−0.41 (−2.57, 2.34)	0.28
V50,%	−0.04 (−1.57, 2.02)	0.07	0.77	0.43	−0.3 (−3.2, 2.4)	0.0001	0.06	−0.6 (−2.63, 1.96)	0.16

IMRT, intensity-modulated (photon) radiation therapy; IMRT, V5. volume (of lung) exposed to 5 Gy or more; d1, dose received by 1% (of the spinal cord).